

# SEISMIC LENS-TYPE SHEAR PANEL DAMPER FOR BRIDGES AND BUILDINGS: INNOVATION AND OPTIMIZATION IN NATURE AND DESIGN TO ENGINEERING FIELDS

**Tatsumasa Takaku\***,  
**Takashi Harada\*\***, **Nobuhiro Yamazaki\*\***, **Tetsuhiko Aoki\*\*\*** and **Yuhshi Fukumoto\*\*\*\***

\*JSCE fellow, Executive Professional Civil Engineer(JSCE), Dr.of Eng.  
1-13-1 Nishikamakura Kamakura Japan 248-0035, [takakut@jcom.zaq.ne.jp](mailto:takakut@jcom.zaq.ne.jp)  
\*\*Nippon Chuzou Co.,Ltd,Kawasaki Japan, \*\*\*Professor emeritus ,Aichi Institute of  
Technology,Toyota Japan, \*\*\*\*Professor emeritus ,Osaka University,Osaka Japan

## ABSTRACT

Experimental study about shear panel was initiated at Fukuyama Univ.( 2005). The paper” Cyclic Shear Behaviour of Low-Yield Steels by New Shear Test Procedure” includes several findings such as:1) shear panel with LY100 is one of the best nature for energy dissipation devices, 2) by strain hardening effect of LY100, plastic zones are spread widely without local stress concentration and which result in well ductility. Then, a variety of bearing types for seismic energy dissipation has been discussed at AIT (2007), and the lens-type shear dampers have been proposed. A number of tests of lens damper have been conducted for practical use at Nippon Chuzou, mainly for highway bridges (2008). Feasibility study project has been started for building application by a group of architects (2013). Lens-type shear panel dampers have been newly developed for highway bridges and buildings against the large-scale earthquakes. It utilizes low yield steel LY100 and concave lens shape panel. Both properties of low yield strength and of high ductility are major requirements for the damping devices. Static and dynamic tests show rectangular shapes of lateral load-displacement hysteresis loops with high quality damping. Damage and life cycles can be estimated by Miner’s rule. Prediction matches well with the testing results. Large deformation of steel with high speed strain rate generates heat of temperature of 300~450°C. Earthquake energy is converted into strain and heat, which results in large energy dissipation.

For application to bridges, both experimental and analytical works have been investigated in parallel. Random loading tests have been examined to evaluate the structural and functional performance of dampers under design level earthquakes, and at the same time to determine the safety margin against collapse under extreme earthquakes. For the evaluation of fracture, two types of prediction formula, damage index method and damage pass method are proposed. For application to buildings, seismic control stud of column type is newly proposed for low/medium-rise buildings with use of low yield steel LY 225.

The design principle of lens damper bases on nature laws of Miner’s rule and similarity laws. An optimization in nature and design to engineering originates in nature law. The truth and beauty are in nature. Results of works are reported.

Keywords: lens-type shear panel damper, bearing, seismic control, bridge, building

# 1. Fundamentals of Lens -type shear panel dampers

## 1-1 Introduction

Static and dynamic tests were conducted to the lens-type shear panel specimens to examine the fundamental behavior of dampers. Several seismic excitations of Level 2 Earthquake specified in Japanese Spec. for Highway Bridges (Part V Seismic Design 2012) are applied to the dampers. At the same time the safety margin against collapse under extreme earthquake events are examined. For fracture evaluation, two types of prediction formula, damage index method and damage pass method are proposed.

## 1-2 Lens-type shear panel damper and half size model (Figure-1.1)

Figure-1.1 illustrates panel details of half size model for test use. Table-1.1 explains mechanical properties of shear panel. In general, a damper is composed of several members, therefore failure mechanism to final collapse are complex. The proposed shear panel is only of single member, consequently, failure is limited in somewhere places inside. In order to get good performance of damper, panel details have been revised by tests.

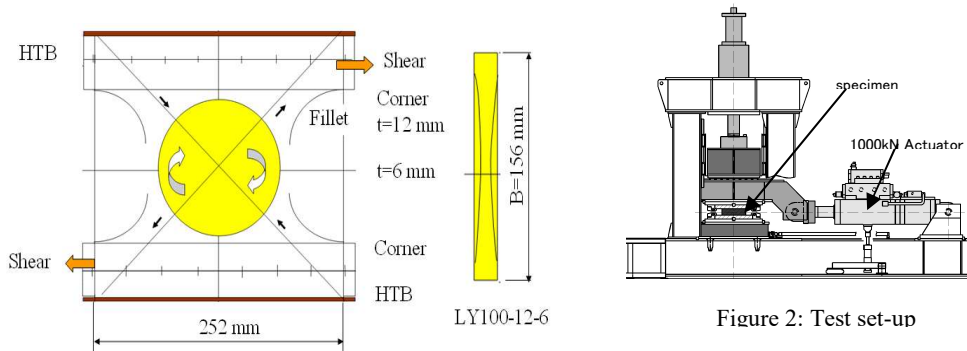


Figure 2: Test set-up  
Figure-1.1 Specimen and test set-up

## 1-3 Specimens and test set-up (Figure-1.1, Table-1.1, Table-1.2)

Nominal mechanical property of panel and low yield steel JFE-LY100 are specified in Table-1.1 and Table-1.2. Test set-up is illustrated in Figure-1.1. Specimen is set to the actuator whose maximum capacity of stroke, velocity, and load are 250mm, 1200mm/s, and 1000kN, respectively. Friction type HTB and a shear key with small clearance of 0.5mm between sole plate, allowing small rotation, are used to connect to the lower and upper set-up beams.

Table-1.1 Mechanical property of half size lens panel LY100-12-6

Yield stress(0.2%strain) $\sigma_y$	80 N/mm <sup>2</sup>
yield displacement(shear strain 3.2%) $\delta_y$	5 mm
yield shear stress $\tau_y = \sigma_y / \sqrt{3}$	46.2 N/mm <sup>2</sup>
yield strength $Q_y$ (at lens center, $t=6$ mm)	66.1 kN
yield strength $Q_y$ (at panel edge, $t=12$ mm)	86.5 kN
Max.shear $Q_{max}$ (at base with fillet)	245 kN
$Q_{max} / Q_y$	2.80 ~ 2.87
$\delta_{max} / \delta_y$	8 ~ 10
$\delta_{max}$	40 ~ 50 mm

Table -1.2 Mechanical property of low yield steel (JFE LY100)

Steel grade	LY-100
Yield strength	80 ~ 120 N/mm <sup>2</sup>
Tensile strength	200 ~ 300 N/mm <sup>2</sup>
Yield ratio	<60%
Elongation	>50%
Charpy value (at 0°C)	>27 J

## 1-4 Static and dynamic loading tests

### Static tests: Gradually increased cycle loading ( $\delta_y \sim 10\delta_y$ , shear strain 3.2% ~ 32%, Table-1.4)

Cyclic lateral load is applied to the top of set-up beam. The increments of shear displacement in each loading cycle are  $\pm \delta_y$ , where  $\delta_y = 5$ mm, which is the shear yield displacement corresponding to

the 0.2% offset yield stress of LY100 (Table-1.1, Table-1.2). The displacement cycles are imposed until collapse at the final stage. One cycle is equivalent to shear strain of 3.2%. In those static loading tests,  $10\delta y$  which is equivalent to shear strain of 32% are recorded at the final stage, where severe cracking damages with large out-of plane twisted deformation are observed. It is left as residual deformation.

**Sinusoidal loading tests: Harmonic motion of SIN wave with various amplitudes (Table-1.3).**

Five different amplitudes (5, 10, 20, 30, 40mm) and four kinds of velocity (slow and time periods of 0.5, 1.0, 2.0 sec) are combined. Slow speed is equivalent to static loading.

**1-5 FUNDAMENTALS OF LENS-TYPE SHEAR PANEL:  
STATIC AND DYNAMIC TEST RESULTS**

**Lens behavior-1: Concave depth and failure modes control (Figure-1.2)**

In general, when flat steel plate increases in thickness, then it increases in strength, reversely decreases in ductility. Lens type shear panel makes the best use of this property, changing thickness with failure modes control. It is so designed to be combination of thicker edge and thin concave that low strength and high ductility are expected with use of low yield steel LY100. Failure mode highly depends on the concave depth. When concave depth is too deep, failure moves from edge to lens center where cross sectional area is smallest in panel. Figure-1.2 shows static test results of various shapes of lens. In static tests of LY100-12-8, LY100-12-6, LY100-12-4, maximum displacements count up to  $8\delta y, 9\delta y, 10\delta y$  in proportion to concave deepness. On the contrary, LY100-12-3 reveals different behavior. It collapsed at edge and center at the same time when maximum displacement is  $8\delta y$ . Early deterioration by crack initiation at lens center was observed. This phenomenon is more clearly observed in dynamic test. Taking safety margin into consideration, LY100-12-6 is recommended to be best use for shear panel dampers.

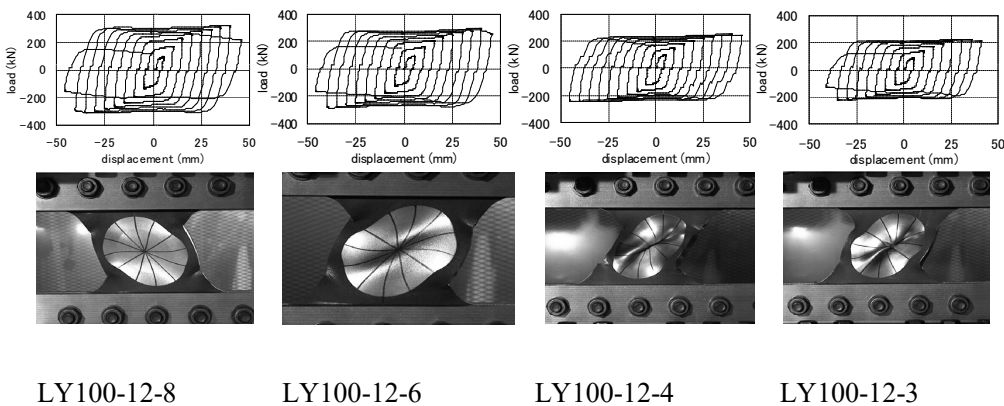


Figure-1.2 Concave depth and failure modes

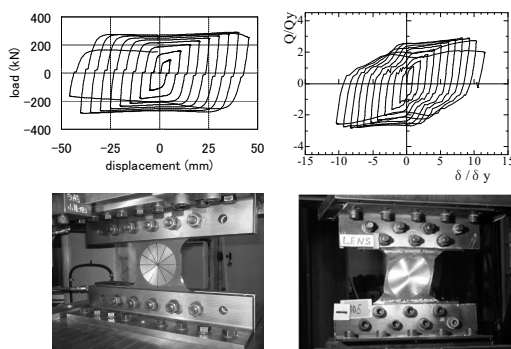


Figure-1.3 Panel connection: Use HTB

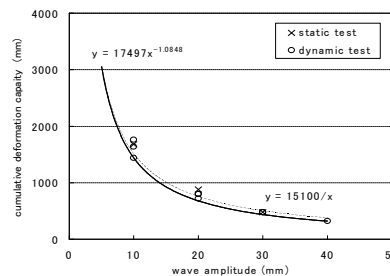
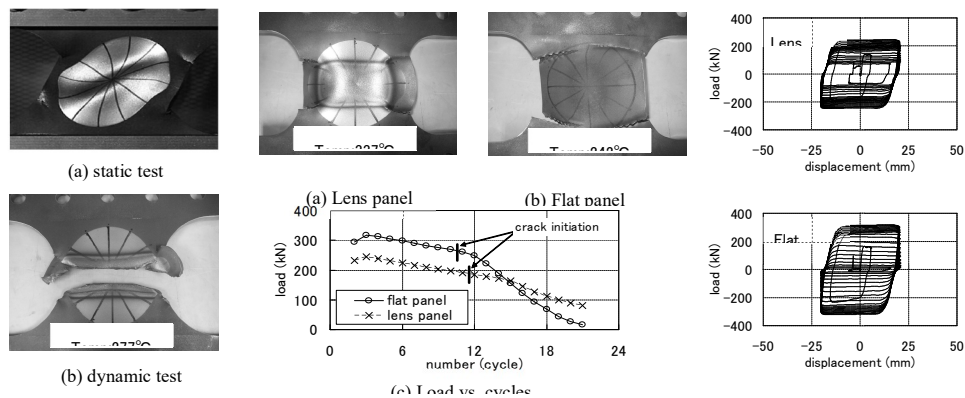


Figure-1.4 Cumulative deformation capacity(mm) /wave amplitude(mm)

### Lens behavior-2: Fillet Corner and failure modes (Figure-1.5)

Fillet corner plays an important role to reduce local stress concentration and consequently, to control failure modes of cracking. When fillet is too large in corner, cracking initiates at lens center. In design sense, it is preferable to fail at four fillet corners for better ductility instead of failure at the horizontal lens center line. Figure-1.5 shows R=6.5t case. In static tests, the peak shear load for R=4t and R=6.5t are 291KN and 330KN, respectively where cracks initiate at the same panel corners. In dynamic test, they show the different type of failure mode. In case R=4t, cracks stay at corners. In case R=6.5t, cracks initiate at center. For R=4t (Figure-1.5(a)), wider plastic zone and higher temperature up (377°C) are recognized than that of R=6.5t, which imply that panel with R=4t has better ductility.

Figure-3.7 shows strain distribution of flat panel with/without fillets.



(sinusoidal test amplitude 20mm)

Figure -1.5: Lens behavior-2: fillet and failure modes R=6.5t

Figure-1.6 Lens behaviour-3: lens panel and flat panel, load versus loading cycles

### Lens behavior-3: Lens panel and flat panel (Figure-1.6)

Figure-1.6 shows the dynamic test results of failure modes for LY100-12-6 (lens) and LY100-12-12 (flat).

In static test, they show the same type of failure mode. In proportion to the area of cross section, shear force is recorded to be 245KN and 315KN, respectively. In contrast, in dynamic test they provide different type of behavior. In case LY100-12-6, plastic zones accompanied with heat radiation spread out widely in radial direction from center to outside, with high temperature 337°C at the surface. In case LY100-12-12, plastic zone is limited into narrow band with not so high temperature 242°C. Figure-5 shows loads versus repeated cycles. After 12 cycles, significant damage at the edges by cracks causes sudden drops of deterioration. Pass of crack propagation left irregularity like gear notch.

### 1-6 Panel connection: Use friction type HTB (Figure-1.3)

Major requirements for connections are as follows:

1. It should transfer seismic lateral forces to shear panel damper so tightly with strong enough rigidity that damping effect is performed completely.
2. Panel edges should be so tightly fixed that it resists both to moment and shear. It is recommended to set double array HTB rather than single arrangement. Single array HTB allows slight rotation due to moment, which results in hinge connection.
3. At ultimate state of failure, cracking in tension state is more crucial than buckling in compression state. Friction type HTB is available to reduce stress concentration with less local constraints. Large deformation causes big thickness change in 3-dimensional direction so that it results in cracking at constrained points such as welding deposits.

Figure-1.6 shows panel behavior connected by single (Case A) and double (Case B) array HTB. In Case A and B,  $Q_{max}/Q_y=2.8\sim 2.87, 2.8\sim 2.90$ , and  $\delta_{max}/\delta_y=9, 10$ , respectively. Note that boundary

changes both strength and ductility. Since size of specimen is limited to small one by loading frame and actuator, half size model with single array HTB are planned in this project (Case B was tested in AIT).

### 1-7 Analytical model: Bilinear model with rectangular loop shape by static and dynamic tests (Figure-1.7)

Figure-1.7 shows the typical load-displacement hysteresis curves by sinusoidal tests with amplitude  $a=30\text{mm}$  (two cases of slow and  $T=1\text{sec}$ ) and an analytical model proposed. Both of them are approximately rectangle with the same peak loads and the same stiffness. Figure-1.7 also shows starting cycle of cracks, from where resistance and stiffness gradually decrease without sudden deterioration, cracking starts at 6 cycles in static and dynamic loadings. For analytical model, a bilinear model of rectangular shape (Figure-2.4), where only two parameters of  $Q_{\max}$  and  $S_1$  are defined, is proposed in Figure-2.4. As maximum loads,  $Q_{\max}$  and  $Q_{\text{peak}}$  are determined;  $Q_{\max}$ , for analytical model, is average values of resistance shears, and  $Q_{\text{peak}}$ , for design use, is the highest value among them.  $Q_{\text{peak}}/Q_{\max}$  is about  $1.13\sim 1.18$ , both in static and dynamic tests.  $S_1$  is slope of stiffness of rectangular shape which is determined by download gradients.  $Q_{\max}, Q_{\text{peak}}, Q_{\text{peak}}/Q_{\max}, S_1$  are determined to be  $245\text{K}, 282\text{KN}, 1.15$  and  $140\text{KN/mm}$ , respectively.

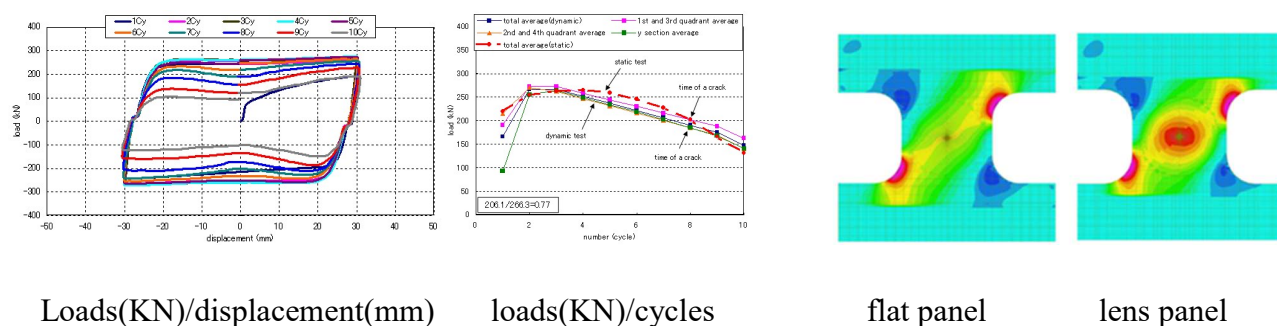


Figure-1.7 load-displacement curves by sinusoidal tests with  $a=30\text{mm}$ , Strain distribution at fillet/ center (flat/ lens, by 2D FEM analysis)

### 1-8 cumulative deformation capacity (CDC): Sinusoidal test results: CDC and damage index (figure-1.4, Tble-1.3)

Table -1.3 Sinusoidal test results and cumulative deformation capacity, damage index  $1/N_f$

amplitude	period	velocity	Cyc. to	$C_f^*$	limit disp.	critical disp.	num.of cycles	damage index
$x(\text{mm})$	$T(\text{sec})$	$v(\text{mm/s})$	failure $C_f$	$d/4x$	$d$	$x*d(\text{mm}^2)$	$y=15100/x$	$N_f=15100/4x^2$
5	1	31	170	168	3360	16800	3020	151
10	2	31	38	36	1440	14400	1510	37.8
10	1	63	46	44	1760	17600	1510	37.8
10	0.5	126	43	41	1640	16400	1510	37.8
15	1	94	17	15	900	13500	1007	16.8
20	1	126	12	10	800	16000	755	9.4
20	0.5	251	11	9	720	14400	755	9.4
30	2	94	6	4	480	14400	503	4.2
30	1	188	6	4	480	14400	503	4.2
30	0.5	377	6	4	480	14400	503	4.2
40	1	251	4	2	320	12800	378	2.4
nominal(avelage) values for design								
18.875	1			10.6	800	15100	800	10.6
								0.094

Table-1.3 shows test results (11 cases) which deal with CDC and number of cycles to failure  $N_f$  versus wave amplitude  $x$  (5, 10, 15, 20, 30, 40 mm). Figure-1.4 draws relation between cumulative deformation capacity ( $y$ , CDC) and wave amplitude ( $x$ ).

$$y = 17497 x^{-1.0848} \quad (1)$$

$$xy=15100 \quad (2)$$

Equation (1) is derived from test data by the minimum square-root method. Equation (2) is simplified formula of lens identity which means that the strain energy capacity is reserved in constant. Based upon Miner's rule, number of cycles to failure  $N_f$  and damage index  $D_f$  are determined by follows.

$$N_f = 15100 / 4x^2 \quad (3)$$

$$D_f = 1/N_f \quad (4)$$

Miner's rule says that design criterion to failure is defined as follow:

$$\sum(1/N_f) < 1 \quad (5)$$

For example, in Table-1.3, when damper is subjected to harmonic motion with the nominal amplitude  $x=18.875\text{mm}$ , its survival number of cycles  $N_f$  and damage index  $D_f$  are 10.6 and 0.094, respectively.

By using the analytical data of traveled pass  $D_{tp}$ , the damage pass  $D_{tp}^*$  is defined as follow:

$$D_{tp}^* = \sum(\text{damage pass coefficient } e) * (\text{response amplitude } x) = \sum(4x^2/18.875) \quad (6)$$

where  $e=x/18.875$ , CDC ( $C_{dc}=800\text{mm}$ ) is evaluated as follow:

$$\sum(D_{tp}^* / 800) < 1 \quad (7)$$

CDC is evaluated by two kinds of methods: 1) damage index method by Eqs.(3), (4) and (5), 2) damage pass method by Eqs.(6) and (7). Both results in the same answer exactly, because they stand on the same base of formula (2). Damage index method have an advantage to be able to evaluate damage state without determination of cumulative pass limit. A trial simulation is shown in Table-1.4.

### 1-9 Gradually increased cycle loading tests : Cumulative deformation and design limit (Table-1.4)

Table-1.4 shows gradually increased loading test results and evaluation of CDC by damage index method and damage pass method. At  $7\delta y$ , cumulative damage index  $\Sigma(1/N_f)$  becomes to be 0.927, almost at final collapse state of 1. In static, maximum displacement counts up to  $9\delta y$  with travelled pass 900mm. In dynamic, it is estimated that maximum displacement reduces to  $7\delta y$ , when damaged travelled pass is 741mm, a little below the cumulative deformation limit value of 800mm. Design criterion can be safely proposed that  $D_s$ (static maximum displacement),  $D_d$ (dynamic maximum displacement),  $D_{tp}$ ,  $D_{tp}^*$ , are determined to be less than 45mm( $9\delta y$ ), 35mm( $7\delta y$ ), 900mm, 800mm, respectively.

Table-1.4 Gradually increased cycle loading tests: cumulative deformation and design limit

loading	amplitude	Trav. pass $\Sigma(4x)$	damage index method			damage pass method			
	$x(\text{mm})$		$N_f=15100/4x^2$	$1/N_f$	$\Sigma(1/N_f)$	$e=x/18.875$	$e*x$	$Q=\Sigma(4e*x)$	$P=Q/800$
$\delta y$	5	20	151.0	0.007	0.007	0.265	1.32	5.3	0.007
$2\delta y$	10	60	37.8	0.026	0.033	0.530	5.30	26.5	0.033
$3\delta y$	15	120	16.8	0.060	0.093	0.795	11.92	74.2	0.093
$4\delta y$	20	200	9.4	0.106	0.199	1.060	21.19	158.9	0.199
$5\delta y$	25	300	6.0	0.166	0.364	1.325	33.11	291.4	0.364
$6\delta y$	30	420	4.2	0.238	0.603	1.589	47.68	482.1	0.603
$7\delta y$	35	560	3.1	0.325	0.927	1.854	64.90	741.7	0.927
$8\delta y$	40	720	2.4	0.424	1.351	2.119	84.77	1080.8	1.351
$9\delta y$	45	900	1.9	0.536	1.887	2.384	107.28	1509.9	1.887
design limit	35	900			$\Sigma(1/N_f) < 1$			800	$P < 1$

## 1-10 Energy dissipation by heat transfer

Large deformation with high speed strain rate generates heat in steel. The heat generation mechanism of the dampers is not yet solved theoretically in our research. Observations and comments are only described.

1. Heat was generated only in dynamic test, not in static test. Slight temperature up was observed in random loading test.
2. Between the time period of 0.5 and 2 seconds, no remarkable difference of heat-up temperature was observed, keeping 350~450°C at the panel surface.
3. Plastic zone and heat radiation spread out widely in the radial direction from lens center to the outside.
4. Cracking delay was observed. It seems that expansion due to heat releases from the stress concentration. Heat transfer contributes to energy dissipation, and consequently good ductility is expected.
5. In the random loading, recorded temperature up is only 40~50°C, which means that seismic behavior subjected to real earthquake is close to static behavior rather than the dynamic one.
6. The deterioration of iron (Table-1.2) by the temperature rise (350~450°C<650°C) was not observed. The thermal expansion causes delay of crack initiation due to less hardness.

## 1-11 Random loading tests

### Test planning (EQ, amplification factor)

Full scale bridge model with dampers are normalized and dynamic analyses are conducted to get the test data. Based upon the fundamentals and analytical data, random loading test programs are planned. Three-types of Level 2 specified earthquakes (EQ2-2-1, EQ2-2-2, EQ2-2-3) and their amplification factors ( $s=1.0, 1.2$ ) are combined into 6 cases for comparison.

### Random test results: Comparison with analysis (Qmax, Qpeak) (Figure-1.8, Table-1.5)

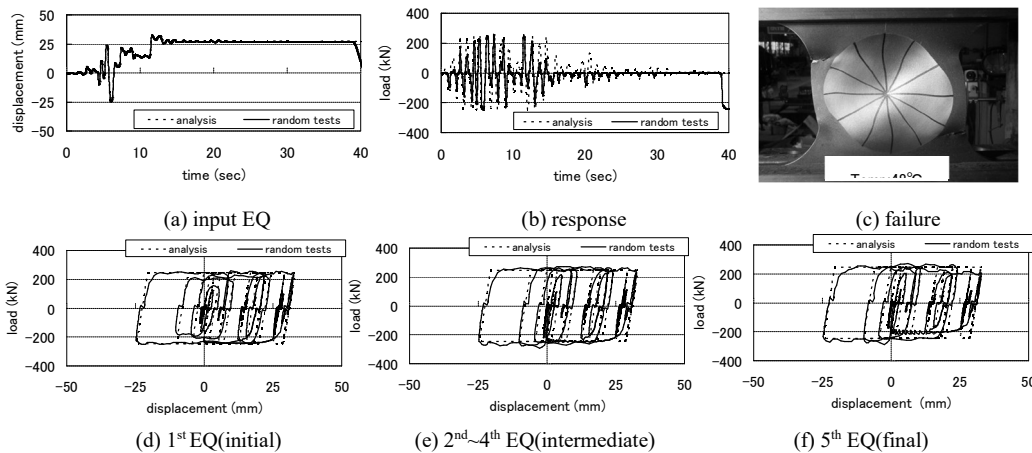


Figure-1.8 Repeated random loading (level-2, EQ2-2-1,  $s=1.2$ ) test results, Time history

Figure-1.8 shows the analytical and test results which explain the time-history of displacements, and the shear resistance of  $Q_{max}$ ,  $Q_{peak}$ , and shear force versus displacements.

1. Displacement of time history: Loading is applied to the damper by the displacement control, and therefore input to actuator should be equivalent to output records exactly.
2. Resistance of time history ( $Q_{max}$ ,  $Q_{peak}$ ): Damper stiffness model is based upon the hysteresis curves in the static tests and the analytical model is assumed to be rectangular shape. In half size model,  $Q_{max}$  and  $Q_{peak}$  are determined to be 245KN and 282KN ( $Q_{peak}/Q_{max}=1.15$ ), respectively. Time history of response verifies that the damper shear resistance is always within  $Q_{peak}$  keeping in the safety zones.

### Random test results: strength (safety margin) and endurance (life cycle)

Table-1.5 summarizes the endurance test results by the repeated random loading. Eight cases of combination with Level-2 EQ (EQ2-2-1, EQ2-2-2, EQ2-2-3) and the amplification factors ( $s=1.0, 1.2$ ) are described. In each case, the test results and the prediction data are compared with each other. In the test, the maximum /minimum displacements, and the number of cycles to failure ( $c_1, c_2$ ) are

counted, where  $c_1$ ,  $c_2$  are the observed cycles when crack initiates ( $c_1$ ) and when it reaches to collapse at the final state ( $c_2$ ). Average (life) cycle  $cf=(c_1+c_2)/2$  is used for comparison with the prediction data. As the prediction data, the damage index method and damage pass method are used. Test data of life cycle  $cf$  matches well with prediction value  $N_f$  within small extent of deviation. As design criterion, it is proposed that  $N_f$  is greater than 3, which means that the damper should survive until at least three times of Level 2 earthquakes. In fact, big earthquakes always accompany with the middle class earthquakes in sequence at the same site in a few days, without loss time of fixing. It requires that at least  $N_f$  should be greater than 2 with enough safety margin. Shear panel connected by HTB is so designed as to repair easily in a short time once damages are found.

Table-1.5 Random loading test results and comparison with failure prediction mm

Case	damper model	random loading level-2 EQ	s	test results: response and cf			prediction by Dtp* and Nf		
				cf	max.disp.	travel.pass	Dtp*	800/Dtp*	Nf
E1	A	EQ2-2-1	1	4.5	33.6	325.1	183	4.37	4.37
E2	A	EQ2-2-2	1	5.5	22.9	321.5	160	4.99	4.99
E3	A	EQ2-2-3	1	5.5	14.8	235.3	123.9	6.46	6.46
E4	A	EQ2-2-1	1.2	3	40.3	390.1	263.3	3.04	3.04
E5	A	EQ2-2-2	1.2	4.5	27.5	386	229.3	3.49	3.49
E6	A	EQ2-2-3	1.2	4.5	17.8	265.2	177.1	4.52	4.52
E7	B	EQ2-2-1	1.2	4.5	33.1	332.6	182.9	4.37	4.37
E8	B	EQ2-2-1	1	6	27.6	272.6	124.8	6.41	6.41
estimate1	B	EQ2-2-1	1.2		33.1	327.1	179.7	4.45	4.45
estimate2	B	EQ2-2-1	1.46		40.3	398.0	266.0	3.01	3.01

damper model: A; Qmax=225KN, S1=134KN/mm, Qeak=259KN, B; Qmax=245KN, S1=140KN/mm, Qpeak=282KN, Dtp\*: damage pass  
s: amplification factor, estimate: scaled by a parameter (s) on the basis of E8(s=1)

**Influence of amplification factor s to dynamic response: Dtp\* and Nf are scaled by s<sup>2</sup>**

Displacements and traveled pass are simply scaled by s, on the other hand, damage pass Dtp\* and Nf are scaled by s<sup>2</sup>. Table-1.5 shows estimated values of response. Nf is easily estimated by a parameter s.

**1-12 Size effects: Both strength and endurance depend on scale of lens prototypes**

Figure-1.9 shows cumulative deformation capacity(CDC)/average dynamic shear strain. Figure-1.10 shows strength/prototype size (LY100-12-6, LY10018-9, LY10024-12). Size effects exist, resulting from non-linearity of behaviours at large deformation. The increase in panel thickness with the size-up raises the hardness of steel plates, then strength increases, reversely ductility decreases.

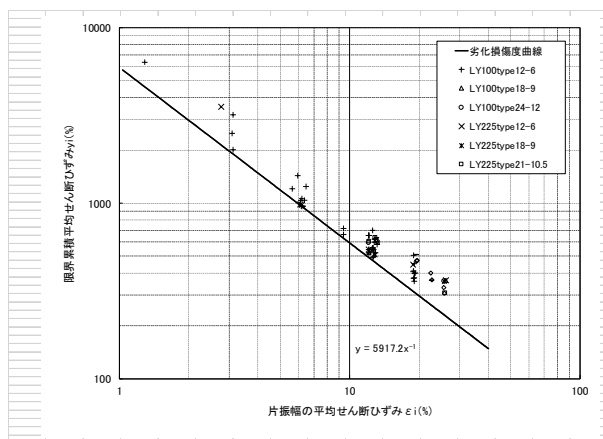


Figure- 1.9 Size effects (endurance, life cycle): measured by average shear strain%

Cumulative deformation capacity/one half wave amplitude (refer to Figure-1.4)

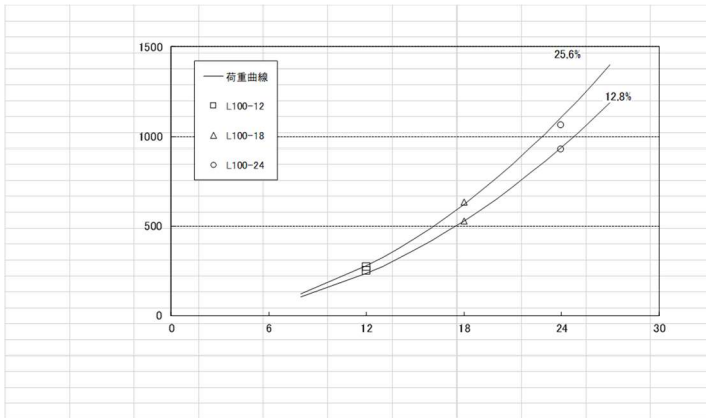


Figure-1.10 Size effects (strength/strain rates) ,Resistance(KN)/damper size(mm)

## SUMMARY

1. Shear panel damper is available as a part of function-separated bearing system. The damper only supports the lateral earthquake forces, and its performance is completely free from vertical bearing shoes. It can be easily maintained once damaged by earthquake.
2. As shear panel damper, lens shape +low yield steel LY100 are most effective way to satisfy the minimum requirements of the dampers. Low strength and high ductility with large energy dissipation are expected.
3. Large deformation of steel with high speed strain rate provides new findings in this research: two items are crucial:1) cumulative deformation capacity, 2) energy dissipation by heat transfer. Both are of great importance to be investigated in future. Size effects exist. The increase in panel thickness with the size-up raises the hardness of steel plates, then strength increases, but ductility decreases.

## 2 Application for highway bridges

### 2-1 Lens-type shear panel dampers and scale-up products (Table-2.1, Figure-2.2)

Based upon the fundamentals of half size model, a prototype model is planned to actual service use by scale-up rules. The size scale-up ratios from the specimen to the actual product is from 0.5 to 0.75~1.0(full size)~1.25, and proportionally the force scale-up ratios change from 25tf to 75~100(full size)~150tf per single unit. The mechanical properties and the fundamental nominal values for design use are specified in Table-1.1.It is possible to make thickness of lens panel with LY100 change by 1mm up from 18mm to 30mm. Lens panel name, LY100-t1-t2 means low yield steel of grade 100, thickness t1 at panel edge and t2 at lens center, lens deepness t2/t1 is set up to be 0.5 as the optimum size ratio.

### 2-2 Setting plan to bridge (Figure-2.1)

Figure-2.1 illustrates damper types of single panel and double panels. Double panels are set up with single panel together in parallel, which possesses double capability of single panel. The lower side of the panel is tightly fixed to the basement by double array HTB with double angles and the upper side is connected by shear key to the sole plate welded to the bottom flange of bridge. The small clearance at shear key connection allows slight rotation due to live loads and small slide due to expansion by the temperature change. Dampers are available both to simply supported bridges and to continuous span bridges with hinge connection to each pier within the limited span length where thermal expansion is well treated.

Table-2.1 lens-type shear panel dampers(LY100), properties

properties		symbol	unit	specimen			products			
specimen & product	standard	product name	strength	tf	25tf	50tf	75tf	100tf	125tf	150tf
		scale	s		0.5	0.75	0.875	1	1.125	1.25
		lens-type shear panel	LY100-t1-t2		L-12-6	L-18-9	L-21-10.5	L-24-12	L-27-13.5	L-30-15
Lens	panel size	thickness at edge	t1	mm	12	18	21	24	27	30
		thickness at center	t2	mm	6	9	10.5	12	13.5	15
		diameter	D	mm	130	195.0	227.5	260.0	292.5	325.0
lens properties	dimensions	square panel B*B	B	mm	156	234	273	312	351	390
		fillet R	4t1	mm	48	72	84	96	108	120
		thickness ratio	B/t1		13	13	13	13	13	13
	strength & displacement	yield strength	Qy	KN	86.49	194.6	264.9	346.0	437.9	540.6
		max./yield ratio	Qmax/Qy		2.83	2.83	2.83	2.83	2.83	2.83
		peak strength	Qpeak	KN	282	635	864	1128	1428	1763
		peak/max. ratio	Qpeak/Qmax		1.15	1.15	1.15	1.15	1.15	1.15
		max.strength (ave.)	Qmax	KN	245	551	750	980	1240	1531
			Qmax	tf	25	56	77	100	127	156
		gradient of unloading	S1	KN/mm	140	210	245	280	315	350
yield displacement	$\delta y$	mm	5	7.5	8.8	10.0	11.3	12.5		
design limit	limit of disp.(max.)	Dmax=7 $\delta y$	mm	35	52.5	61.25	70	78.75	87.5	
	limit of disp.(peak)	Dpeak=8 $\delta y$	mm	40	60	70	80	90	100	
	limit of damage pass	Dtp*	mm	800	1200	1400	1600	1800	2000	

### 2-3 Damper model: Bilinear model with rectangular loop shape (Figure-1.7, Figure-2.4)

Figure-1.7 shows the typical load-displacement hysteresis curves for 30mm constant amplitude under the sinusoidal tests (two cases of slow and T=1sec). The peak load gradually decreases with repeated cycles and the cracking initiates at 7~8 cycles. Figure-2.4 shows an assumed analytical model, a bilinear model of rectangular shape, where two parameters of Qmax and S1 are defined. The maximum loads, Qmax and Qpeak are determined; Qmax for analytical model denotes the average value of resistance shears, and Qpeak for design use is the highest value among them. Qpeak /Qmax is about 1.04~1.18, both in the static and dynamic tests. S1 is determined from the unloading gradients. On the basis of static and dynamic database, two damper models are proposed.

(1) S-model: Stiff model of hard response. Use for strength design. The values of Qmax-s, Qpeak-s and S1-s are determined to be 245KN, 282KN and 140KN/mm, respectively.

(2) R-model: Regular model of soft response. Use for displacement design and life cycle evaluation. The values of Q max-r, S1-r are set to be 225KN and 134KN/mm respectively, which are equivalent to 92% and 96% values of S-model.

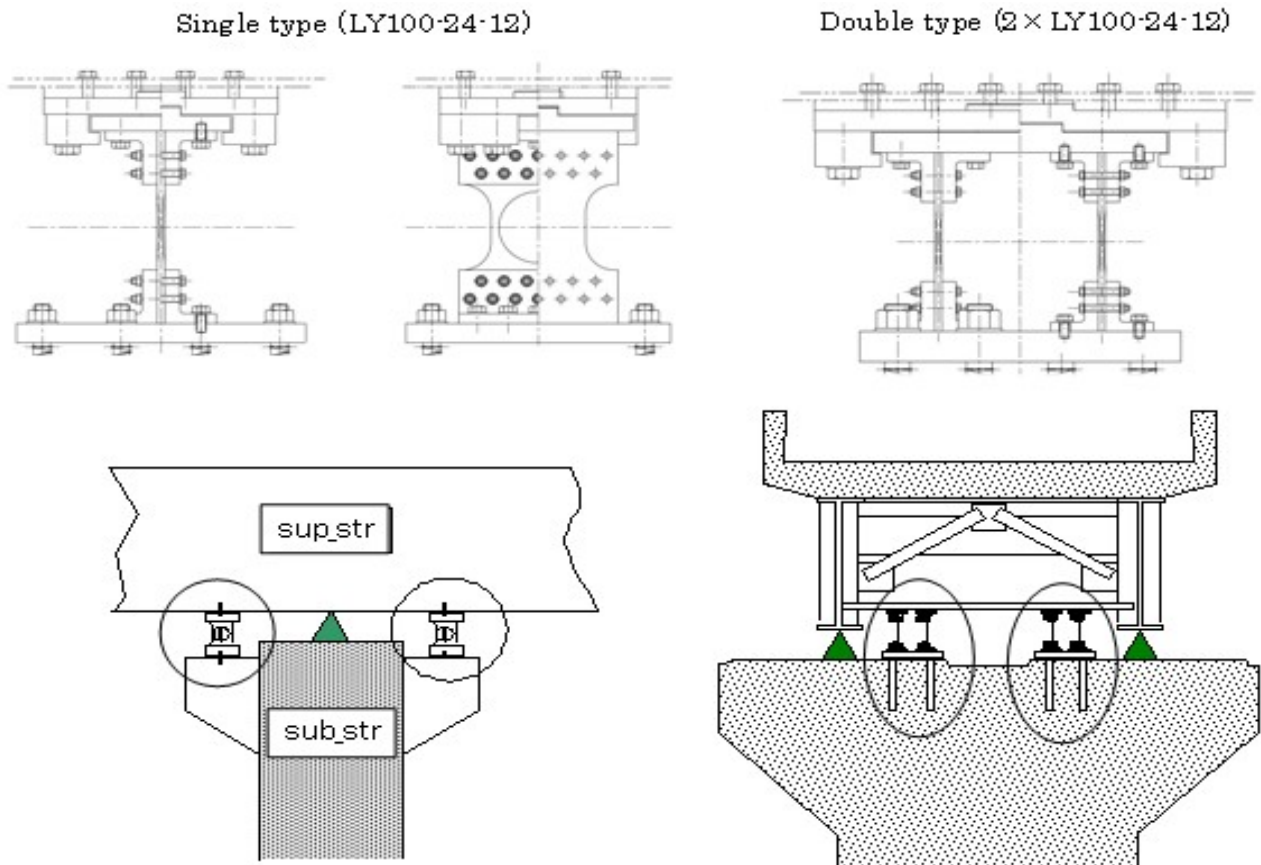


Figure- 2.1 Set up of lens damper to bridges

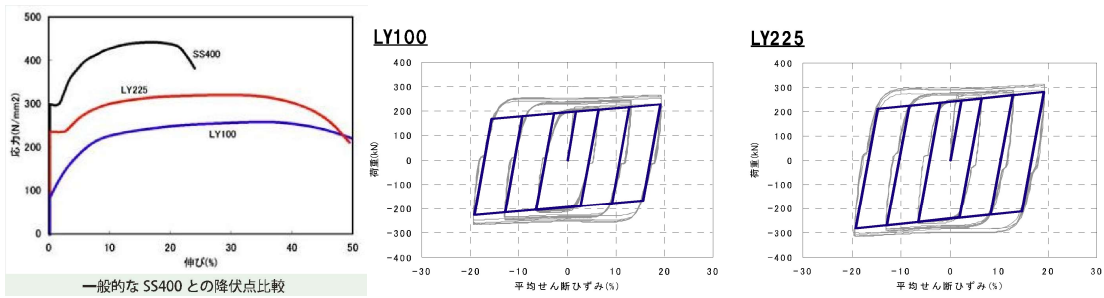
#### 2-4 Low yield steels (LY100, LY225) and damper properties (Figure-2.2)

Two kinds of low yield steel are available in Japanese steel market. LY 100 is for flexible use in bridge fields. LY225 is rather for rigid use in building field. Both elongations are up to 50%.

type		LY100 type12-6	LY100 type18-9	LY100 type21-10.5	LY100 type24-12	LY100 type27-13.5	LY100 type30-15	
shear resistance		KN	220kN	510kN	690kN	900kN	1150kN	1420kN
scale			1.00	1.50	1.75	2.00	2.25	2.50
shape	h (effective height)	(mm)	156	234	273	312	351	390
	T (thickness)	(mm)	12	18	21	24	27	30
	φ ( diameter of Lens)	(mm)	130	195	228	260	293	325
property	k <sub>1</sub> ( primary rigidity)	(kN/mm)	70	105	123	140	158	175
	k <sub>2</sub> (secondary rigidity)	(kN/mm)	1.078	1.617	1.887	2.156	2.426	2.695
	Q <sub>y</sub> (yield load)	(kN)	198.1	445.7	606.7	792.4	1002.9	1238.1
	Q <sub>max</sub> (maximum load)	(kN)	227.4	511.6	696.4	909.6	1151.2	1421.2
	δ <sub>y</sub> (yield displacement)	(mm)	2.83	4.25	4.95	5.66	6.37	7.08
	δ <sub>max</sub> ( maximum displacement)	(mm)	30.0	45.0	52.5	60.0	67.5	75.0
	maximum shear strain%		±19.2%	±19.2%	±19.2%	±19.2%	±19.2%	±19.2%
Q <sub>d</sub> ( design load)	(kN)	295.6	665.1	905.3	1182.4	1496.5	1847.5	

type		LY225 type12-6	LY225 type18-9	LY225 type21-10.5	LY225 type24-12	LY225 type27-13.5	LY225 type30-15	
shear resistance		KN	280kN	630kN	860kN	1120kN	1420kN	1760kN
scale			1.00	1.50	1.75	2.00	2.25	2.50
shape	h (effective height)	(mm)	156	234	273	312	351	390
	T (thickness)	(mm)	12	18	21	24	27	30
	φ ( diameter of Lens)	(mm)	130	195	228	260	293	325
property	k <sub>1</sub> ( primary rigidity)	(kN/mm)	70	105	123	140	158	175
	k <sub>2</sub> (secondary rigidity)	(kN/mm)	1.337	2.006	2.340	2.674	3.008	3.343
	Q <sub>y</sub> (Yield load)	(kN)	246.4	554.4	754.6	985.6	1247.4	1540.0
	Q <sub>max</sub> (Maximum load)	(kN)	281.8	634.1	863.0	1127.2	1426.6	1761.3
	δ <sub>y</sub> (yield displacement)	(mm)	3.52	5.28	6.16	7.04	7.92	8.80
	δ <sub>max</sub> ( maximum displacement)	(mm)	30.0	45.0	52.5	60.0	67.5	75.0
	maximum shear strain%		±19.2%	±19.2%	±19.2%	±19.2%	±19.2%	±19.2%
Q <sub>d</sub> ( design load)	(kN)	366.3	824.3	1121.9	1465.4	1854.6	2289.7	

#### Mechanical properties of LY100 and LY225



yielding(N/mm<sup>2</sup>)/elongation(%)

Loading(KN)/average shear strain(%)

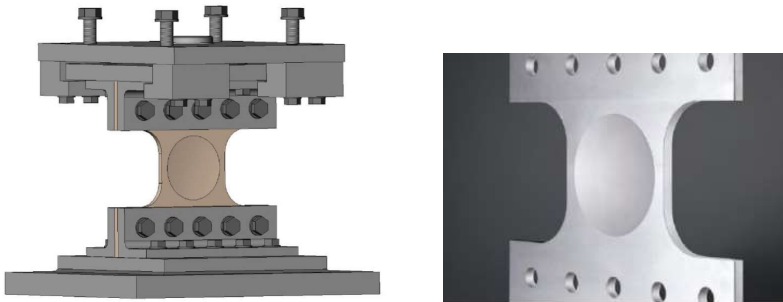


Figure-2.2 Line-up of lens dampers(LY100/LY225 ) and mechanical properties

### 2-5 Dynamic response with S-model and R-model: Testing, analysis and reviews (Table-2.3, Table-1.5(E1~E8))

Table-2.3 shows the analytical and test results on the 3-span continuous bridge (Figure-2.5) with S-model and R-model dampers, subjected to Level-2 EQ-2-2-1. When base shear ratio  $f=Q_{max-r}/Q_{max-s}$  is given to be  $f=0.918$ ,  $E1/E8$  of max.displacement, traveled pass of moving distance are roughly estimated proportionally to  $1/f^2$ . When damper stiffness becomes soft, the displacement increases as much as double of the scale factor  $f$ . E4, E7model with EQ amplification factor  $s=1.2$  shows the same tendency as E1, E8 models. In both cases,  $Q_{max}$  is kept in constant. Increase in EQ amplification factor  $s$  and decrease in stiffness  $Q_{max}$  of the dampers cause increase in the displacement, which are dependent on  $s$  and  $f$  values, where  $s$  is equivalent to  $f^2$  as the response sensibility factor.

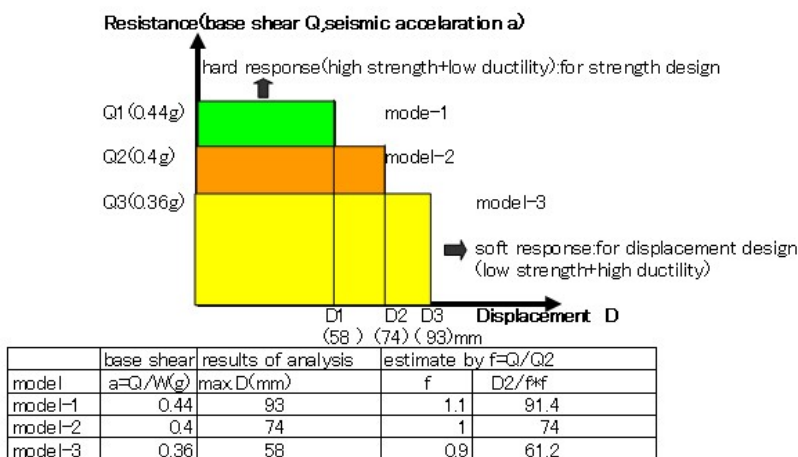


Figure-2.3 Resistance-displacement: soft/hard response

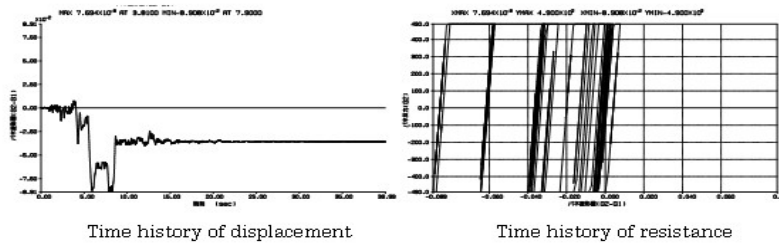
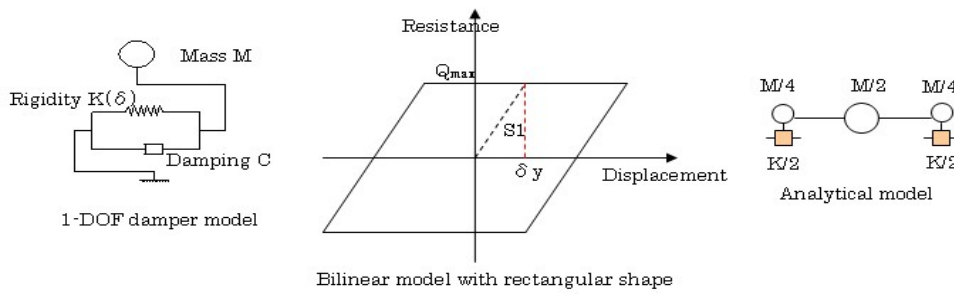


Figure-2.4 Analytical model of 1-DOF and response

Table-2.2 Dynamic response with S-model and R-model: Testing/analysis and design reviews (model:3-span continuous bridge with dampers, Figure-2.6~2.8)

test case <sup>5)</sup>	damper model type	shear stiffness	EQ2-2-1 disp.scale s	random loading test results			analysis by output data		Effects of $f=Q_{max}/Q_0$ and $s$ to response					
				Max.disp D	trav.pass Dtp	life cycles (c1+c2)/2	damage pass Dtp*	life cycles Nf	shear ratio f	Max.disp $D \cdot f^2$	trav.pass $Dtp \cdot f^2$	d.pass $Dtp^* \cdot f^4$	life cycles $Nf/f^4$	$Nf \cdot s^2/f^4$
E1	S	245	1	27.6	272	6	125	6.40	1	27.6	272	125	6.40	6.40
E8	R	225	1	33.6	325	4.5	183	4.37	0.918	28.3	274.1	130.2	6.15	6.15
E4	S	245	1.2	33.1	332	4.5	183	4.37	1	33.1	332.0	183.0	4.37	6.30
E7	R	225	1.2	39.2	390.1	3	263	3.04	0.918	33.1	329.0	187.1	4.28	6.16

$Nf=800/Dtp^*$ , c1:cycles at crack initiation, c2:cycles at failure, s: displacement amplification factor of EQ2-2-1 loading

Table-2.3 Resistance/displacement (Q: base shear)

Item	Resistance	response	$Q_{max}, Q_{peak}$	$(Q/Q_0) f$	$(Dtp) 1/f^2$	$(Dtp^*) 1/f^4$
$Q_{peak}$ (test results)	Disp. control loading KN	hard	245~282	1	1	1.000
	Force control loading KN	soft	225~258	0.912	1.203	1.448
Base shear (design)	Base shear acc.0.44g	hard	0.44	1.000	1	1.000
	Base shear acc.0.40g	soft	0.4	0.909	1.235	1.525
Damper model (analysis)	S-model $Q_{max}$ KN	hard	245	1.000	1	1.000
	R-model $Q_{max}$ KN	soft	225	0.918	1.186	1.407

$Q_{peak}/Q_{max}=1.15$  f: base shear ratio

Table-2.4 Results of dynamic analysis: 1-DOF model

Level-2 EQ	Damper	panel	scale	$Q_{max}(KN)$	S1	W(KN)	$Q_{max}/W$	$Q_{peak}/W$	Max.disp	Min.disp	Dtp*	Df	$Nf=1/Df$
EQ2-2-1	S-model	L-23-11.5	0.958	900.0	268.3	2450	0.367	0.422	9.7	-123.4	425.8	0.278	3.600
		L-24-12	1.000	980.0	280.0	2450	0.400	0.460	7.7	-89.1	239.3	0.150	6.686
		L-25-12.5	1.042	1063.4	291.7	2450	0.434	0.499	5.6	-60.7	136.6	0.082	12.207
	R-model	L-23-11.5	0.958	828.0	257.6	2450	0.338	0.389	16.4	-146.9	682.1	0.445	2.247
		L-24-12	1.000	901.6	268.8	2450	0.368	0.423	9.6	-119.9	405.1	0.253	3.950
EQ2-2-2	S-model	L-23-11.5	0.958	900.0	268.3	2450	0.367	0.422	25.5	-54.3	148.6	0.097	10.316
		L-24-12	1.000	980.0	280.0	2450	0.400	0.460	20.7	-51.1	106.2	0.066	15.062
		L-25-12.5	1.042	1063.4	291.7	2450	0.434	0.499	7.0	-44.2	75.9	0.046	21.968
	R-model	L-23-11.5	0.958	828.0	257.6	2450	0.338	0.389	11.9	-70.1	202.1	0.132	7.585
		L-24-12	1.000	901.6	268.8	2450	0.368	0.423	25.4	-54.4	141.4	0.088	11.318
EQ2-2-3	S-model	L-23-11.5	0.958	900.0	268.3	2450	0.367	0.422	48.7	-68.7	260.0	0.170	5.896
		L-24-12	1.000	980.0	280.0	2450	0.400	0.460	69.9	-36.0	184.9	0.116	8.653
		L-25-12.5	1.042	1063.4	291.7	2450	0.434	0.499	59.2	-17.4	112.4	0.067	14.839
	R-model	L-23-11.5	0.958	828.0	257.6	2450	0.338	0.389	78.4	-70.0	381.2	0.249	4.021
		L-24-12	1.000	901.6	268.8	2450	0.368	0.423	48.3	-68.6	247.5	0.155	6.465
		L-25-12.5	1.042	978.3	280.0	2450	0.399	0.459	69.6	-36.8	178.5	0.107	9.338

$Q_{peak}/Q_{max}=1.15$

## 2-6 Base shear design: Seismic design with dampers

Ductility capacity is evaluated in terms of cumulative plastic strain. The effects of dynamic loading were examined in reference to the maximum resistance and ductility capacity on the basis of the experimental works.

Two different design approaches are considered in base shear design, one aims at controlling the maximum shear forces transmitted by the dampers to the piers, while the other at controlling the displacement. The former is associated with the pier strength and design of the structural members, and the other is associated with the ultimate displacement capacity, the post-EQ remaining capacity of life cycles and available joint gaps. The design approaches are empirically based on the experimental database.

Several design factors are defined as follows:

Basic seismic acceleration

$$a=Q \text{ (base shear force) } / W \text{ (dead load)}$$

Modified seismic acceleration

$$a^*=q \cdot a, \quad q: \text{ resistance factor}$$

Base shear ratio:

$$f=Q \text{ (base shear force) } / Q_0 \text{ (basic base shear force)}$$

Displacement ratio:

$$g= D \text{ (displacement) } / D_0 \text{ (basic displacement)}$$

For base shear design with use of shear panel dampers, those factors are correlated with each other.

## 2-7 Base shear design: Strength design and displacement design (Figure-2.3)

Concept of the base shear design is shown in Figure-2.3 as resistance (base shear force  $Q$ , seismic acceleration  $a=Q/W$ ) versus displacement. Model-1 indicates hard response with high strength and low ductility, which is for structural design use. Reversely, model-3 indicates soft response with low strength and high ductility, which is for displacement design use. In case of the damper with bilinear model of rectangular shape subjected to random loading,  $Q_{max}$  is kept in constant, whereas displacement changes. Figure-2.3 also shows results of dynamic analysis on 3 cases for  $Q_{max}$  parameters (0.36g, 0.40g, 0.44g). The maximum displacement  $D$  is roughly scaled by  $1/f^2$ , where  $f=0.9, 1.0, 1.1$ , respectively.

## 2-8 Resistance versus displacement: Hard response and soft response (Table-2.3)

Table-2.3 shows resistance versus displacement, associated with laboratory testing methods, base shear design and damper models. Each case has hard response with high strength+low ductility and soft response with low strength+high ductility.

$Q_{peak} / Q_{max}$ : It depends on the laboratory testing methods. When the dynamic loadings are imposed by displacement control method and force control method,  $Q_{peak}$  falls in different value. The displacement control method restrains the input-output displacements by actuators, consequently, the response reactions causes resistance changes, reversely the force control method by the facility of turn table, response reactions causes displacement change. Actual responses at site are thought to be close to soft response with semi rigid boundary. Depending on connection rigidity, the resistance factor  $q= Q_{peak}/Q_{max}$  changes from 1.04 to 1.15.

## 2-9 $Q_{peak}$ , base shear, damper model: Correlation with base shear ratio $f$ (Table-2.3)

Each base shear difference in Table-2.3 is treated by the same parameter  $f$ . Each item has the same level of scale-up factor  $f=0.9$ . For safety design, the resistance force and the displacement should be evaluated equivalently by the different damper models, S-model and R-model, respectively.

**2-10 Base shear design: Design coefficients and design criterion: Qpeak design by Qmax analysis (Table-2.1)**

In principle, by the two types of damper models, dynamic analyses should be simulated for strength design and displacement design. Results are modified by several design coefficients (LY100-12-6).

1) Damper model factor (S-model, R-model)

$$f = Q_{max-s} / Q_{max-r} = 245 / 225 = 1.089$$

2) Displacement amplification factor of EQ

$$s = 1.0 \sim 1.2$$

3) Resistance factor

$$q = Q_{peak} / Q_{max} = 1.04 \sim 1.15$$

4) Peak displacement (by static tests)

$$D_{peak} = 8\delta y = 40\text{mm},$$

Max. displacement (by dynamic tests),

$$D_{max} = 7\delta y = 35\text{mm}$$

When  $D_{tp}^*$  is within the allowable limit 800mm,  $D_{peak} / D_{max} = 1.15$  is allowed.

5) Damage index:

$$D_f = 1 / N_f < 1 \text{ (at ultimate state),}$$

$$D_f < 1/3 \text{ (at service use)}$$

6) Damage pass, Life cycles (number of cycles to failure)

$$D_{tp}^* < 800 \text{ mm, } N_f > 1 \text{ at ultimate state}$$

$$D_{tp}^* < 800/3 \text{ mm, } N_f > 3 \text{ at service use}$$

**2-11 Dynamic analysis by 1-DOF : Base shear design by 1-DOF model (Figure-2.4, Table-2.4)**

Figure-2.4 illustrates 1-DOF (one degree of freedom) model for design simulation. For design use, several parameters are considered.

a) Lens panel size: LY100-23-11.5, LY100-24-12, LY100-25-12.5

b) Basic seismic acceleration  $a = 0.338 \sim 0.434g$ , Modified seismic acceleration  $a^* = 0.4 \sim 0.5g$

c) Damper model: S-model, R-model

d) Level-2 EQ: EQ2-2-1, EQ2-2-2, EQ2-2-3

For each case with design parameter combinations, maximum displacement  $D$ , traveled pass  $D_{tp}$ , damage  $D_{tp}^*$  and life cycles  $N_f$  are shown in Table-2.7, for design use. Basic seismic acceleration  $a = 0.4 \sim 0.5g$  determines critical values of maximum displacement  $D$  and damage

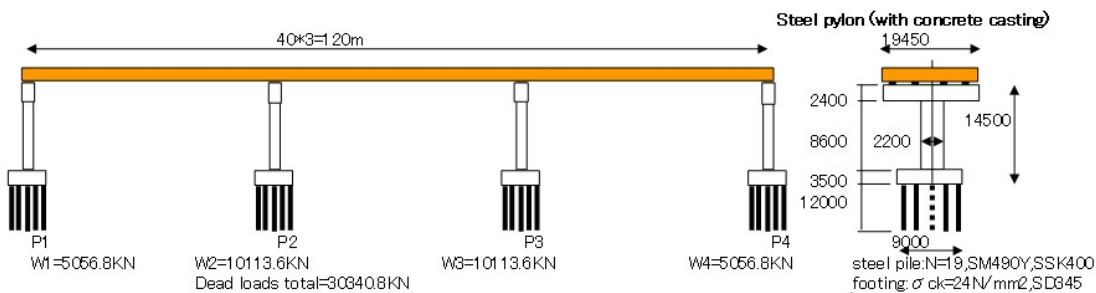


Figure-2.5 Bridge model for analysis: 3-span continuous bridge (width=19.45m)

Table-2.5 Results of dynamic analysis (1-DOF ): Displacement D,Dtp, Dtp\*

by EQ2-2-1, EQ2-2-2, EQ2-2-3 (mm)  
Effects of base shear ratio f to displacements, and average of 3 waves

Level-2 EQ	Damper			Results by dynamic analysis					Effects of base shear ratio f to displacements			
	Damper	panel	scale	Qmax(KN)	D(amplitude)	Dtp	Dtp*	Dtp*/Dtp	f=Qmax/Q0	f' Dtp	f' Dtp*	f' D
EQ2-2-1	S-model	L-23-11.5	0.958	900.0	66.6	952.5	425.8	0.447	0.918	803.4	302.9	56.1
		L-24-12	1.000	980.0	48.4	882.8	239.3	0.271	1.000	882.8	239.3	48.4
		L-25-12.5	1.042	1063.4	33.1	848.5	136.6	0.161	1.085	999.0	189.3	39.0
		Average	1.0	981.1	49.3	894.6	267.2	0.293	1.00	896.7	243.9	47.8
	R-model	L-23-11.5	0.958	828.0	81.6	1105.5	682.1	0.617	0.918	932.2	485.0	68.8
		L-24-12	1.000	901.6	64.7	948.5	405.1	0.427	1.000	948.3	404.9	64.7
		L-25-12.5	1.042	978.3	48.5	874.6	230.8	0.264	1.085	1029.5	319.8	57.1
		Average	1.0	902.6	65.0	976.2	439.3	0.436	1.00	978.2	403.2	63.6
EQ2-2-2	S-model	L-23-11.5	0.958	900.0	39.9	528.7	148.6	0.281	0.918	445.9	105.7	33.7
		L-24-12	1.000	980.0	35.9	490.3	106.2	0.217	1.000	490.3	106.2	35.9
		L-25-12.5	1.042	1063.4	25.6	442.2	75.9	0.172	1.085	520.7	105.2	30.1
		Average	1.0	981.1	33.8	487.1	110.2	0.223	1.00	488.2	105.7	33.2
	R-model	L-23-11.5	0.958	828.0	41.0	603.6	202.1	0.335	0.918	509.0	143.7	34.6
		L-24-12	1.000	901.6	39.9	527.1	141.4	0.268	1.000	527.0	141.3	39.9
		L-25-12.5	1.042	978.3	36.2	481.4	102.3	0.212	1.085	566.6	141.7	42.6
		Average	1.0	902.6	39.0	537.4	148.6	0.272	1.00	538.5	142.2	39.0
EQ2-2-3	S-model	L-23-11.5	0.958	900.0	58.7	763.3	260.0	0.341	0.918	643.8	184.9	49.5
		L-24-12	1.000	980.0	52.9	710.1	184.9	0.260	1.000	710.1	184.9	52.9
		L-25-12.5	1.042	1063.4	38.3	656.3	112.4	0.171	1.085	772.7	155.7	45.1
		Average	1.0	981.1	50.0	709.9	185.7	0.257	1.00	711.5	175.2	49.2
	R-model	L-23-11.5	0.958	828.0	74.2	871.4	381.2	0.437	0.918	734.8	271.1	62.6
		L-24-12	1.000	901.6	58.5	759.1	247.5	0.326	1.000	759.0	247.4	58.5
		L-25-12.5	1.042	978.3	53.2	699.8	178.5	0.255	1.085	823.8	247.4	62.6
		Average	1.0	902.6	61.9	776.8	269.1	0.340	1.00	778.4	255.3	61.2
Average of 3 waves	S-model		1.0	981.1	44.4	697.2	187.7	0.258	1.0	698.8	174.9	43.4
	R-model		1.0	902.6	55.3	763.4	285.7	0.349	1.0	765.0	266.9	54.6

$$D=(\max.\text{disp}+\min.\text{disp})/2$$

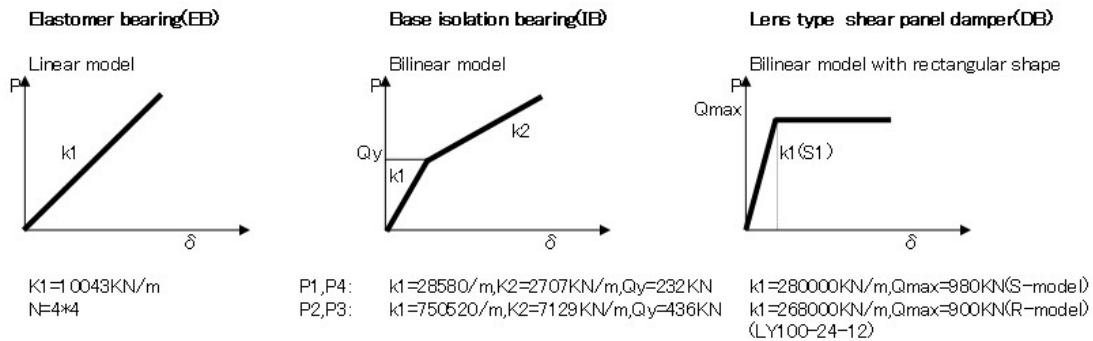


Figure-2.6 Analytical model of bearings

3-continuous span bridge mode(40m\*3=120m) (Figure 7,B)



	Bearing		P1	P2	P3	P4	Amax(g)	Apeak(g)	remarks
Case-1	Elastomer	number	4*EB	4*EB	4*EB	4*EB			conventional method
	EB	disp.	196	196	197	195	0.789		soft rigidity+large displacement
Case-2	Isolator	number	4*IB	4*IB	4*IB	4*IB			base isolator system
	IB	dis.	261	161	161	271	0.602		long period+large displacement
Case-3	ED+DB	number	4*EB	4*DB	4*DB	4*GB			combined use,movable at end support
	ED+DB	disp.	155	43	43	155	0.496	0.572	due to temperature expansion
Case-4	Damper	number	4*DB	4*DB	4*DB	4*DB			damper system,small disp with large
	DB	disp.	64	55	59	53	0.388	0.446	energy dissipation

Damper (DB with S-model):LY100-27-135(case3),LY100-24-12(case-4)

Amax,Apeak:seismic acceleration at P2

Figure-2.7 Results of dynamic analysis with various types of bearings)

Case study 1: Comparison with elastomer (EB), base isolator (IB) and damper (DB)

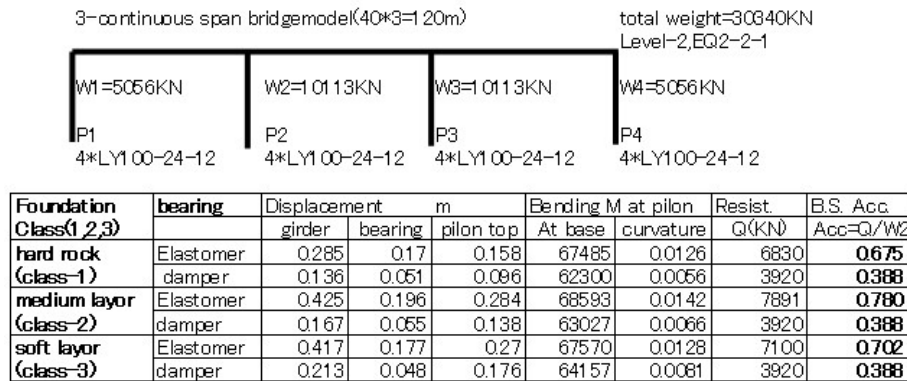


Figure-2.8 Case study-2 : Foundation rigidity (Class-1, 2, 3 foundations): response at P2

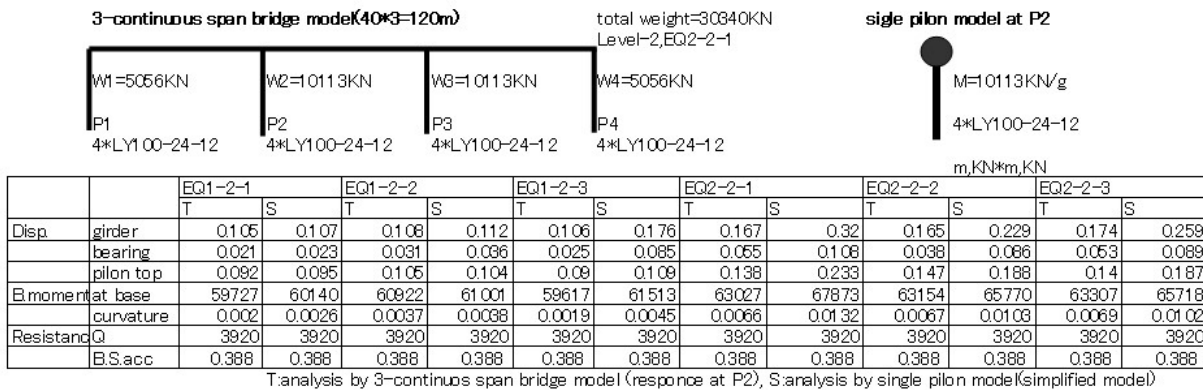


Figure-2.9 Case study-3: Dynamic analysis by exact model and simplified model

pass  $D_{tp}^*$ .  $N_f$  changes widely from 2.25 to 21.97, dependent on level-2 EQ. In design, the average values of 3 waves are evaluated for safety margin.

**2-12 Displacement design: Evaluation of D,  $D_{tp}^*$  and  $N_f$  by R-model (Table-2.2, Table-2.5)**

Table-2.2 shows the displacement D, the traveled pass  $D_{tp}$  and the damage pass  $D_{tp}^*$  of 1-DOF model, which is based on the results of the dynamic analysis (Table-2.5). It is important to analyze and pick up the wave amplitudes correctly and exactly from the random time history response. An amplitude of random vibration wave is so determined to be the distance between a top point of velocity zero and a bottom point of velocity zero where the wave velocity returns reversely that velocity response curves are required together with the displacement response curves to analyze the data correctly.  $D_{tp}$  is the moving distance of response in which noises are cut off, whereas  $D_{tp}^*$  is damaged distance which is proportional to the square of each amplitude. It is clear that big difference of  $D_{tp}^*$  exists between EQ2-2-1, EQ2-2-2 and EQ2-2-3, and S-model and R-model. The average values of  $D_{tp}^*$  with S-model are 277,110,186mm for EQ2-2-1, EQ2-2-2 and EQ2-2-3, respectively. The average values of 3 waves are 188 and 285mm for S-model and R-model, respectively.

Table-2.5 shows the effects of the base shear ratio  $f$  to the displacements. When the base shear ratio  $f$  ( $Q_{max}/Q_0$ ) is given, dynamic responses of displacement D, traveled pass  $D_{tp}$ , the damage pass  $D_{tp}^*$  are estimated to be proportional to  $1/f^2, 1/f^2$  and  $1/f^4$ , respectively.

Table-2.2 shows the effects of  $f$  and  $s$  to response. In each case of E1, E8, E4 and E7,  $N_f \cdot s^2 / f^4$  converges to the original value of  $N_f = 6.40$  of E1, where  $f = 1, s = 1$ .

## 2-13 Numerical analysis:3-span continuous bridge

### Analytical model: superstructure+pier+foundation (Figure-2.5, Figure-2.6)

An analytical model with steel bridges, steel pylons of concrete casting inside and steel piles is illustrated in Figure-2.5. Dimensions of member properties and dead weight are roughly described. For case studies, 3 types of bearing, elastomeric bearing (EB), base isolation bearing (IB) and damper bearing (DB) are prepared with four sets for each support. Linear or bilinear models of each bearing are shown in Figure-2.6. The bridge is supported by bearings with hinge connection against the seismic forces.

#### A. Case study-1: Bearing types and damping effects (Elastomer, Base isolator, Damper) (Figure-2.7)

Case-1 (Elastomer): Conventional bearing system provides large displacement of 196 mm (at P2) and large base shear acceleration of 0.79g almost without damping effect.

Case-2 (Isolator): Base isolation system provides large displacement of 261mm (at P1), 161mm (at P2) and reduced lateral forces of 0.602g as counter effects.

Case-3 (Elastomer (P1, P4) +damper (P2, P3)): It is combined use with EB and DB (LY100-27-13.5), movable at end supports (P1, P4) due to temperature expansion. It provides small displacement of 43mm (at P2, P3) and 155mm (at P1, P4), totally reduced base shear acceleration of 0.496g at P2.

Case-4 (Damper): Damper system (LY100-24-12) provides small displacement of 55mm (at P2) and reduced base shear acceleration 0.388g (at P2) with large energy dissipation. Four damper arrangements at P1, P4 contribute to the base shear reduction at P2, P3 with desirable seismic load distributions.

#### B. Case study-2: Foundation rigidity (Class1,2,3), On soft layer and hard rock (Figure-2.8)

Foundation rigidity classes are provided by the design code, Class1 (hard rock), class2 (medium layer) and class3 (soft layer). Analytical results of bridges with dampers (DB) and elastomers (EB), displacement, bending moment and resistance at p2 are shown in Figure-2.8. Displacements at girders and pylon tops vary from 136, 167, 213mm, and 96, 138, 176mm, respectively, which proportionally lead to the rigidity change from hard to soft foundation. On the contrary, the displacements at dampers are almost kept in constant about 48~55mm, with the same resistance. Since the damper stiffness is relatively rigid more than that of piers and foundation, dynamic sensibility to foundation rigidity is thought to be substantially small.

#### C. Case study-3: Dynamic analysis by the exact models and single pylon model (Figure-2.9)

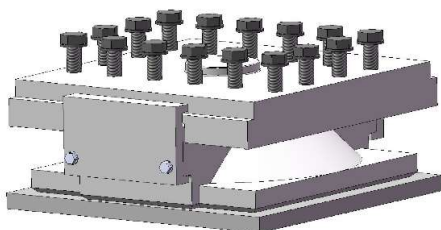
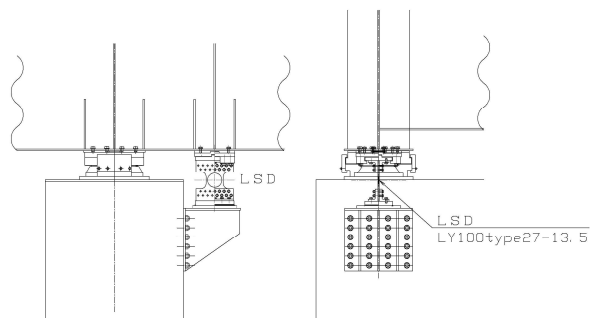
At the initial stage of damper plan, rough estimate design methods are required in a global sense. Figure-2.9 compares the exact analytical results with rough estimate by use of simplified model, subjected to Level-1 (EQ1-2-1, EQ1-2-2, EQ1-2-3) and Level-2 (EQ2-2-1, EQ2-2-2, EQ2-2-3) design EQ in the Code. A simplified model is created at P2 partially, in a form of simply cantilever column, independent from other portions. When subjected to Level-1 EQ, no difference is observed between exact and simplified model. On the other hand, Level-2 EQ makes a big difference of about twice displacement. When subjected to Level-2 big EQ, total seismic base shear is shared by each support equally, and the seismic loads are distributed without concentration to rigid piers. Even though a simplified model provides rough estimate with safety side, finally exact analysis will be required.

## 2-14 Retrofit project : Ohgishima Bridge( at JFE iron works, Kawasaki Japan,2010 )

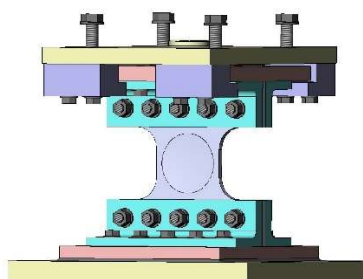
Bridge type:3-span continuous bridge(36+36+36=108m),4- I section girder type.

Seismic control device: Lens-type shear panel damper, 4\* LY100-27-13.5(one side at the fixed pier)

Bearing: Function separated type, rubber bearing(existing)+ seismic control devices(retrofits).



**Bearing**



**Lens-type shear panel damper**

**Figure-2.10 Retrofit work by bridge damper (Ohgisima Bridge, Kawasaki)  
(by courtesy of JFE Steel)**

## SUMMARY

1. Lens-type shear panel damper is developed as a part of function-bearing system to serve for lateral seismic loads, and it provides easy maintenance with panel parts change once being damaged.
2. Base shear design method is proposed based on the damper model with bilinear model with rectangular loop shape. A simple model of 1-DOF provides principal and practical data to design use. Base shear acceleration of the bridge with shear dampers goes down to 0.4~0.5g from 0.78g of elastomeric bearings and from 0.6g of base isolation system.
3. Large deformation of low-yield steel with high speed strain rate causes two crucial problems; 1) cumulative deformation capacity against fracture, and 2) energy dissipation by heat transfer. Base shear design should evaluate resistance versus displacement and life cycles precisely for safety and serviceability.
4. Modified seismic acceleration design (MSAD) methods is simply proposed based on the dampers identity of bilinear model with rectangular loop shape. MSAD is composed of two parts: strength design for structural members and displacement design for fracture evaluation of the dampers

### 3. APPLICATION FOR BUILDINGS

#### 3-1 Seismic control stud type: Multi-story low /medium-rise steel buildings

Lens-type panel damper has been developed for highway bridges at the beginning of 2007, and then the similar lens-type damper was extended to steel buildings. The Lens Damper Renovation Council was organized in 2013 to develop the lens-type shear panel dampers of seismic control stud (column type) system for the low and medium rise steel buildings.

#### Advantages for residential buildings (figure-3.1)

1. As compared with other conventional dampers, the system becomes simpler, then the number of parts, assembling man-hour and finally the cost can be reduced.
2. The stud system does not block off sight of windows and the opening spaces like cross bracings.
3. Once earthquake damages occur, it is easy to exchange the damaged parts to new parts quickly. Besides, the systems can retrofit to improve safety on the present buildings.
4. Either outside set-up or inside set-up of the dampers can be chosen considering usage and safety from the residential requests.

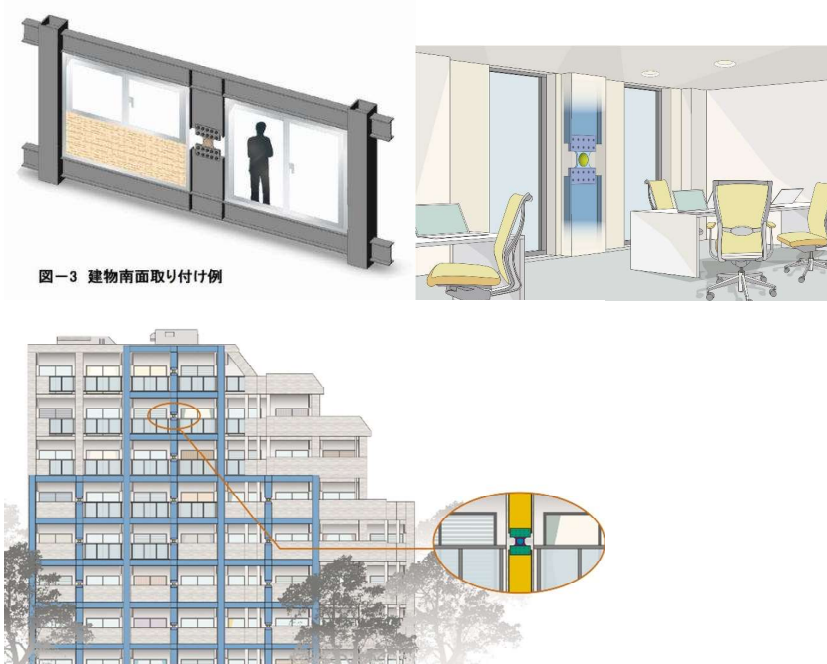


Figure-3.1 Seismic control stud with lens-type panel damper  
( by courtesy of Lens Damper Renovation Council)

#### Planning on damper size: one size for one floor in principle

One and the same size of the same property should be installed on each floor. The number of dampers(N) on each floor is simply calculated from the total base shear capacity divided by the shear capacity of one damper. When the two different size

dampers are allocated on one floor, the smaller size damper is damaged bigger than the large one, and thus the life time becomes short. From a view point of endurance period, the bigger damper is better and should be installed in concentration.

### **New building construction project (Tokyo,2015), (Figure-3.2)**

Building: 6F steel frame building, new construction

Damper arrangement:2F(LY225-22-11),3F(LY225-19-9.5),4F(LY225-16-8)  
5F(LY225-12-6), X-Y each direction

Setting: Seismic control stud type for each floor (one same size for one floor)



**Figure- 3.2 New building construction works (Tokyo)**  
(by courtesy of Lens Damper Renovation Council, [www.tekken.co.jp/tech/](http://www.tekken.co.jp/tech/))

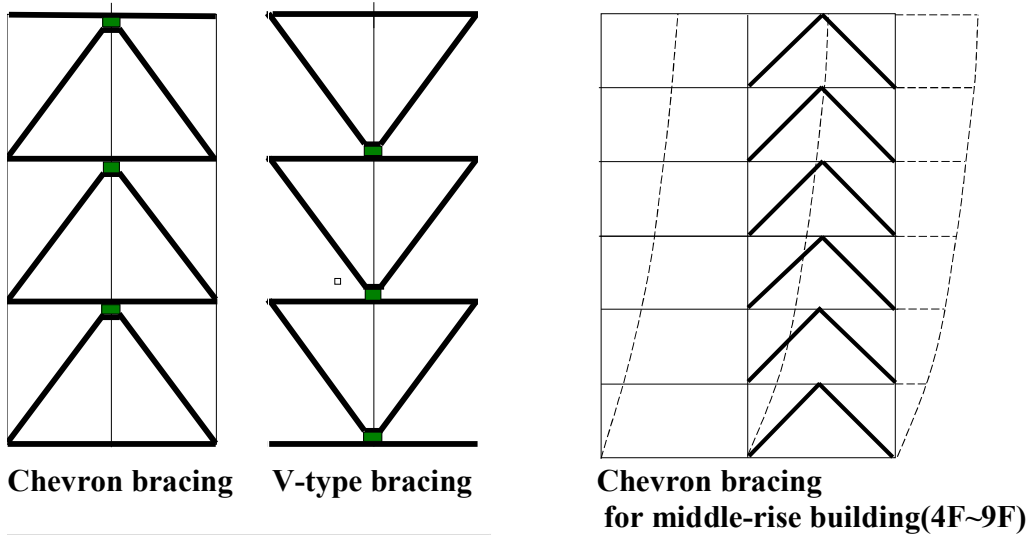
### **3-2 Chevron bracing: Residential house and low/medium-rise building with bracing Seismic behaviour of chevron bracings without dampers**

Despite their poor seismic performance, the use of chevron (reverse-V) braced frames still represents a very popular means of resisting lateral loads in steel building structures. Under severe earthquake ground motions, the braces are expected to buckle and lose their compressive strength. The beams are then pulled downward due to the combined action of the gravity loading and the tension acting braces. Unless the beams are designed to carry this net vertical load together with the axial loads that develop from the braces, a plastic hinge eventually forms at mid-span of the beams before the tension braces reach their yield tensile capacity. This behaviour results in a severely pinched hysteretic lateral response with strength and stiffness deterioration, which can lead to the formation of fragile storeys in multi-storey frames.

### **Innovative use of lens-type shear panel dampers with chevron bracing Chevron bracing damper (Figure-3.3, Figure-3.5)**

As supplementary energy dissipation devices, the lens-panel dampers are useful for the seismic force resisting system. The effective use of dampers attached to the chevron bracing provides not only additional damping to the structure but also a period shift like base isolation. The use of dampers results in the efficiency of the seismic control system, which significantly reduce the linear seismic forces induced on the structure without

devices. Control of the displacements is also achieved, which is highly dependent on the initial value of damping in the structure without devices. Installing dampers into the bracing significantly improves their seismic performance by keeping their elastic behavior.



drift control	base shear control
flexible system	rigid system
middle rise build.	low rise build.
ductility design	strength design

Figure- 3.3 Braced buildings with /without damper



Figure-3.4 Chevron bracing with viscous damper, Chevron braced building (Yokohama)

**Proposal of chevron bracing damper: lens-type damper +viscous damper (Figure-3.5)**

As supplementary dampers, the viscous dampers are installed at the ends of the horizontal bracing for stoppers against the large displacement which results in rigid frame as braking system (Figure-3.4). Instead of the viscous devices, rubber pads are available as sliders on one side. Configuration of damping system changes from being flexible within design state to being rigid at the ultimate state against overturning (safety guard, fail safe).

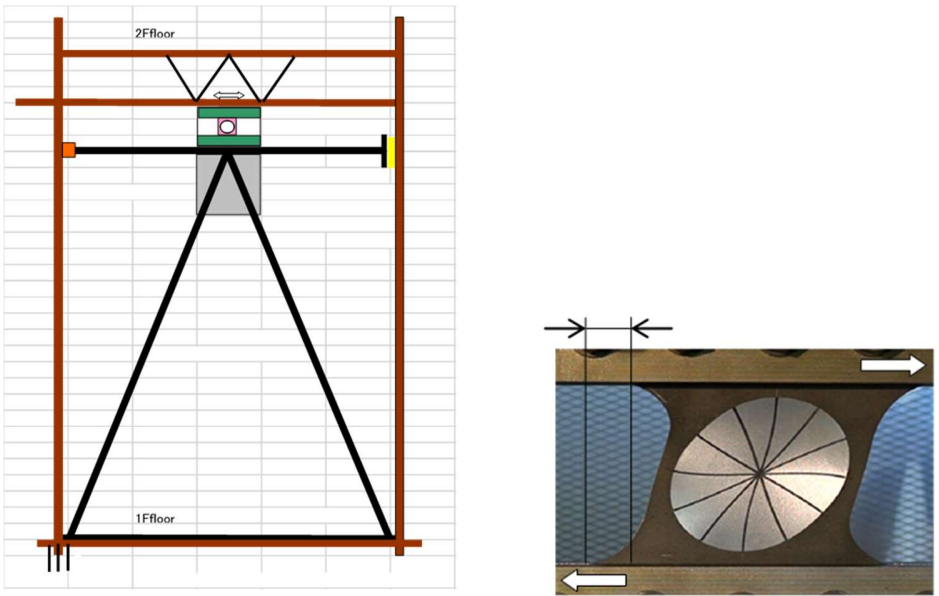
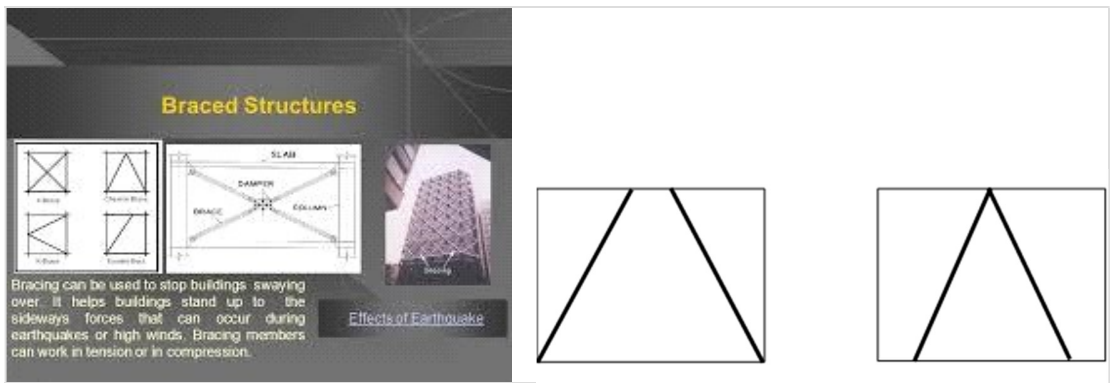


Figure-3.5 Seismic control chevron bracing with lens-type damper and viscous damper (Interlayer drift control by shear damper+ excessive drift stopper)

**3-3 Other bracings: Friction damper in center of X-type cross bracing (Figure-3.6)**

The friction dampers are designed not to slip during wind. During a major earthquake, they slip prior to yielding of structural members. In general, the lower bound is about 130% of wind shear and the upper bound is 75% of the shear at which the members will yield. When the slip load is very low or high, the response is very high. Optimum slip load gives the minimum response. Selection of slip load should ensure that after an earthquake, the building return to near the original position under the elastic action of structure. Eccentricity of bracing system causes the secondary moment at the gusset plates. The local twisted deformation of the gusset plate results in energy dissipation.



Seismic eccentrically braced frames  
Figure-3.6 Friction Dampers with X-type bracing and others (by internet data)

### 3.4 Damage monitoring system for shear panel damper(Figure-3.7)

#### Image data processing by digital camera and FEM analysis

Image data processing method has been studied for damage monitoring of shear panel dampers by AIT in 2007. The original purposes of research are : 1) observation of strain distribution of shear panel by image data processing of camera, 2) observation of relationship between strain distribution and damper properties. The method is available widely for visible observation of panels as monitoring tools.

#### Flow chart of experimental works

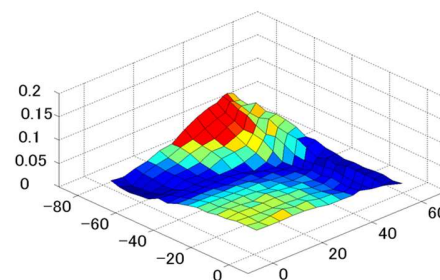
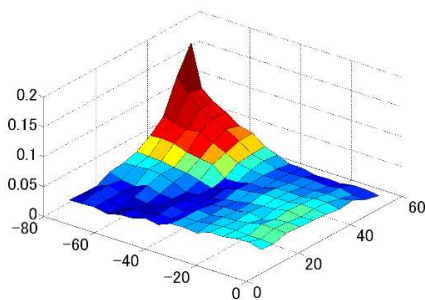
- 1) Photography : the image making with the digital camera(positioning the mesh points before/after loadings)
- 2) Image processing: tracking/digitizing/labeling, noise reduction, array formation for FEM
- 3) FEM analysis: calculation of displacement/cumulative strain with compatible image data.

#### Specimens, test set-up and digital camera

- 1) Specimens: a) rectangle flat panel (156\*156\*6mm, SS400) without fillet  
b) rectangle flat panel (156\*156\*6mm, SS400) with fillet (corner R=36mm)
- 2) The specimen and test set-up resemble those in Figure-1.1. In front of the specimen, two set of digital cameras are fixed.
- 3) Image data processing is limited within a quarter partition of the rectangle panel.
- 4) Figure-3.7 shows strain distribution of the panels, where only a quarter symmetry partition is drawn (center at (0,0)). Strain distribution is measured by equivalent cumulative strain.

#### Work results

- 1) Shear strain by image data processing matches well with shear strain by strain gauges.
- 2) It is useful to estimate the durability and the present life age of the damaged dampers due to the past earthquakes.
- 3) Fillet corner plays an important role to control failure modes of cracking (Fugure-1.6).



Rectangle panel (156\*156\*6,SS400) without fillet      Rectangle panel with fillet(R=36mm)

Figure-3.7 Strain distribution of rectangle panel , 2D FEM analysis with image data processing of a quarter symmetry partition(center(0,0)), x-y axis(mm)/z axis:equivalent cumulative strain(Mi)

## CONCLUSIONS

1. The shear panel damper of lens-type shape+ low yield steel LY100/LY225 are the effective use to satisfy the minimum requirements of dampers. Low strength and high ductility with large energy dissipation are obtained from the present results.
2. Large deformation of steel with high speed strain rate provides new findings: 1) cumulative deformation capacity against fracture, 2) energy dissipation by heat transfer. Both are the important topics to further investigation.
3. Shear panel damper is available as a part of function-separated bearing system. The damper only supports the lateral earthquake forces. It provides easy maintenance with panel parts change once being damaged.
4. Base shear acceleration of the bridge with shear dampers goes down to 0.4~0.5g from 0.78g of elastomeric bearings and from 0.6g of base isolation system.
5. Seismic control stud type damper is available for multi-story low/medium rise steel buildings. Either outside set-up or inside set-up of the dampers can be chosen considering usage and safety for the residential requests.
6. Chevron (reverse V) bracing with lens-type shear panel damper is effective for independent seismic force resisting system. As supplementary dampers, when viscous dampers are installed in addition, it plays the stopper role against the large displacement as a braking system.
7. Similarity law of damper shape: Size effects exist, resulting from non-linearity of behaviours at the large displacement. Size-up prototype shows to be stronger but fragile.

**The truth and beauty are in nature, and optimization in nature and design originates in nature laws.**

## REFERENCES

### FUNDAMENTALS AND BRIDGES

- Uenoya, M., Fukumoto, Y., Nakamura, M. and Ishida, S. (2005). Cyclic Shear Behaviour of Low-Yield Steels by New Shear Test Procedure, Proc. of the 1<sup>st</sup>International Conference on Advances in Experimental Structural Engineering, Nagoya, June 2005,183-188.
- Public work research center.(2006). Bridge dynamic seismic design manuals, fundamentals and applications of dynamic analysis and seismic design, May 2006, part2, page 88~109.
- Aoki,T.,Liu,Y.,Takaku,T.,Uenoya,M.,and Fukumoto,Y.(2007).Experimental investigation of tapered shear type seismic devices for bridge bearings.*Proc.,8th Pacific Structural Steel Conference (PSSC)*,New Zealand, March 2007.1,111-117.
- Liu,Y.,Aoki,T.,Takaku,T.,and Fukumoto,Y.(2007).Repeated cyclic loading test of lens-type shear panel dampers with low yield steel. *JSCCE Structure engineering, Proceeding Vol.53A*,2007,3.
- Aoki,T., Liu,Y.,Takaku,T.and Fukumoto,Y.(2008).A new type of shear panel dampers for highway bridge bearings. *EUROSTEEL2008*,3-5, September 2008, Graz, Austria.

- Takaku, T., Aoki, T., and Fukumoto, Y. (2008). CONTROL DEVICE OF VARIABLE-THICKNESS SHEAR PANEL FOR BRIDGE, Toko Engineering Consultants, Co., Ltd, Patent- 4162693, 2008.08.01
- Ishiyama, M., Yamazaki, N., Harada, T., Takaku, T., Imai, Y. and Aoki, T. (2009). Experimental static Evaluation of lens-type shear panel dampers with LY100. JSCE annual conference, Proceeding Vol.64, I-042, 2009, 9.
- Yamazaki, N., Ishiyama, M., Harada, T., Takaku, T., Imai, Y. and Aoki, T. (2009). Experimental dynamic Evaluation of lens-type shear panel dampers with LY100. JSCE annual conference, Proceeding Vol.64, I-043, 2009, 9.
- Imai, Y., Takaku, T., Aoki, T., Ishiyama, M., Yamazaki, N. and Harada, T. (2009). Seismic behaviour of 3-span continuous girder bridge with lens-type shear panel dampers. JSCE annual conference, Proceeding Vol.64, I-044, 2009, 9.
- Aoki, T., Dang, J., Zhang, C., Takaku, T., and Fukumoto, Y. (2009). Dynamic shear tests of low-yield steel panel dampers for bridge bearing. Proc. of 6<sup>th</sup> International Conference of STESSA 2009, 16-20 August 2009, Philadelphia, USA.
- Takaku, T., Harada, T., Aoki, T., and Fukumoto, Y. (2010). Design and experimental performance evaluation of lens-type shear dampers for highway bridge bearings, Proc. of 9th Pacific Structural Steel Conference October 19-22, 2010, Beijing, China, 1175 - 1186.
- Takaku, T., Chen, F., Harada, T., Ishiyama, M., Yamazaki, N., Aoki, T. and Fukumoto, Y. (2010). Static and dynamic behavior of lens-type shear panel dampers for highway bridge bearing. SDSS'Rio 2010-International Colloquium on Stability and Ductility of Steel Structures, 18~10 September 2010, Rio de Janeiro, Brazil
- Yamazaki, N., Harada, T., Ishiyama, M., Takaku, T., Imai, Y. and Aoki, T. (2010). Experimental performance evaluation of lens-type shear panel dampers due to earthquake wave, JSCE annual conference, Proceeding Vol.65, I-554, 2010, 9.
- Ishiyama, M., Yamazaki, N., Harada, T., Takaku, T., Ting, H. and Aoki, T. (2010). Damage evaluation method of lens-type shear panel dampers. JSCE annual conference, Proceeding Vol.65, I-555, 2010, 9.
- Chen, F., Takaku, T., Imai, Y., Yamazaki, N., Harada, T. and Aoki, T. (2010). Seismic design method of lens-type shear panel dampers for highway bridges. JSCE annual conference, Proceeding Vol.65, I-556, 2010, 9.
- Yamazaki, N., Harada, T., Ishiyama, M., Takaku, T., Imai, Y. and Aoki, T. (2011). Size effects of lens-type shear panel dampers, JSCE annual conference, Proceeding Vol.66, I-359, 2011, 9.
- Matsuimoto, S., Harada, T., Ishiyama, M. and Yamazaki, N. (2013). Experimental evaluation about out-of-plane behaviour of lens-type shear panel dampers, JSCE annual conference proceeding, Vol.68, VI-119, 2013, 9.
- Takaku, T. (2016). Performance evaluation system in engineering matters: Systematic and theoretical approach to humanity, ISSS2016, Proceeding, Boulder, Colorado USA, July 23~30, 2016

## **BUILDINGS**

- Subhash C. Goel. (1992). Earthquake Resistant Design of Ductile Braced Steel Structures, Stability and ductility of steel structures under cyclic loading, CRC Press, Inc. 1992
- Nakashima, M. and Wakabayashi, M. (1992). Analysis and Design of Steel Braces and Braced Frames in Building Structures. Stability and ductility of steel structures under cyclic loading, CRC Press, Inc. 1992

- Natori,S.,Kubota,M.,Mishio,Y.,Shirinashihama,S.,Yamazaki,N. and Ishiyama,M.(2013).Development project of Lens-type shear panel damper .Part1-Outline of the program. AIJ annual conference, Proceeding 21418,2013.8
- Yamazaki,N.,Ishiyama,M.,Kubota,M.,Natori,S.,Mishio,Y.and Shirinasihama,S.(2013). Development project of Lens-type shear panel damper. Part2-Experimental evaluation of structural performance. AIJ annual conference, Proceeding 21419,2013.8
- Ishiyama,M.,Yamazaki,N.,Kubota,M.,Abe,T.,Mishio,Y.and Shirinasihama,S.(2013).Development project of Lens-type shear panel damper .Part3- Seismic analysis design model and damage evaluation method. AIJ annual conference, Proceeding 21420,2013.8
- Mishio,Y.,Shirinashihama,S.,Kubota,M.,Abe,T.,Ishiyama,M.and Yamazaki,N.(2013).Development project of Lens-type shear panel damper .Part4- Experimental evaluation of size effect and similarity law . AIJ annual conference, Proceeding 21421,2013.8
- Yamazaki,N.,Ishiyama, M.,Kubota,M.,Natori,S.,Abe,T. and Mishio,Y.(2014). Development project of Lens-type shear panel damper. Part5- Dynamic structural performance evaluation due to random vibration. AIJ annual conference, Proceeding 21420,2014.9
- Ishiyama,M.,Yamazaki,N.,Kubota,M.,Natori,S.,Abe,T. and Mishio,Y.(2014).Development project of Lens-type shear panel damper .Part6- Damage curve evaluation. AIJ annual conference, Proceeding 21420,2014,9
- Mishio,Y.,Kubota,M.,Natori,S.,Abe,T.,Ishiyama,M. and Yamazaki,N.(2014).Development project of Lens-type shear panel damper .Part7- Analytical Evaluation of seismic design model by irregularity wave of the earthquake. AIJ annual conference, Proceeding 21428,2014,9
- Natori,S.,Kubota,M.,Abe,T.,Ishiyama,M.,Yamazaki,N. and Mishio,Y.(2014).Development project of Lens-type shear panel damper .Part8 -Experimental evaluation of out-of-plane deformation problems. AIJ annual conference, Proceeding 21429,2014,9
- Yamazaki,N.,Ishiyama,M.,Someya,Y.,Kubota,M.,Natori,S.,Abe,T.,Mishio,Y.,Isiwatari,Y. and kitajima,K.(2016).Experimental study of Lens-type shear panel damper sustained by stud type column, Part1-Outline of testing and set-up. AIJ annual conference, Proceeding 21058,2016.8
- Someya,Y.,Ishiyama,M.,Yamazaki,N.,Kubota,M.,Natori,S.,Abe,T.,Mishio,Y.,Isiwatari,Y. and kitajima,K.(2016).Experimental study of Lens-type shear panel damper sustained by stud type column, Part2-Testing results of Part-1. AIJ annual conference, Proceeding 21059,2016.8
- Natori,S.,Ishiyama,M.,Yamazaki,N.,Someya,Y.,Kubota,M.,Abe,T.,Mishio,Y.,Isiwatari,Y. and kitajima,K.(2016).Experimental study of Lens-type shear panel damper sustained by stud type column,Part3-Perfoemance evaluation of Part 2 results, AIJ annual conference, Proceeding 21060,2016.8
- Lenz damper renovation council.(2018).[http://lens damper, Lens-type shear panel damper for buildings \(scope/overviews/products/merit/property\), Nippon Chuzou Co.,Ltd, Kawasaki Japan](http://lens damper, Lens-type shear panel damper for buildings (scope/overviews/products/merit/property), Nippon Chuzou Co.,Ltd, Kawasaki Japan).
- Yasaman,B.Sanda,K.and Robert,T.(2018).Seismic Assessment of Existing Steel Chevron Braced Frames.ASCE,J.Struct.Eng..2018,1446(6):04018046.